Monthly Notices
of the
ROYAL ASTRONOMICAL SOCIETY

MNRAS **444,** 2128–2132 (2014) doi:10.1093/mnras/stu1508

One-element interferometer

Ramesh Balasubramanyam★

Raman Research Institute, Sadashivanagar, Bangalore I-560080, India

Accepted 2014 July 25. Received 2014 July 25; in original form 2014 January 23

ABSTRACT

We apply the phase-switching method of Ryle to convert single dish radio telescopes to *one-element interferometers* and thereby accord them the benefit of correlation measurements, viz. to measure only the flux from the celestial sources avoiding contributions from the receiver and the atmosphere. This application has many uses: (a) enables single dishes to image the sky efficiently without the need to scan, measuring all sources, point, extended, spectral and continuum, with both bolometric and coherent receivers; (b) enables adding reliable short-spacing data to existing interferometers such as Atacama Large Millimetre-wave Array,, mitigating calibration issues; (c) enables ground-based NIR/MIR imaging to accurately remove atmospheric contributions; (d) can be adapted to provide an alternate surface measurement method for telescopes.

Key words: instrumentation: interferometers – methods: observational – telescopes.

1 INTRODUCTION

Total power outputs from ground-based single dish telescopes suffer from system gain variations, including $1/f$ noise (e.g. Meinhold et al. 2009), and atmospheric fluctuations. This fundamentally limits imaging faint-continuum sources with single dishes or adding zero and short-spacing data from single dishes to interferometric data. Various techniques such as correlation receiver (Tiuri 1964; Jarosik et al. 2003), beam switching and basket weaving (Haslam, Quigley & Salter 1970; Winkel, Flöer & Kraus 2012) have been developed to mitigate this problem. Joint deconvolution schemes (Cornwell 1988; Sault, Staveley-Smith & Brouw 1996) have been developed that reliably integrate single dish data with the interferometric data set. Heterogeneous arrays also facilitate wide-field imaging with high resolution (Woody et al. 2004). None the less, each technique has some limitation in practice.

Let us look at two instances in astronomy that highlight the importance of short-spacing data: (a) measuring the Sunyaev–Zelodovich effect towards clusters of galaxies (Myers et al. 1997; Birkinshaw 1999; Carlstrom, Holder & Reese 2002); (b) making a spectral index map of a diffuse emission region. In both cases, if wide-spread, low-intensity emission is removed (either by limited position-switching or by spatial filtering of extended emission), the overall emission will be underestimated leading to inaccurate conclusions. For example, one may derive the spectral index map from $\frac{S_{\nu 1}-\delta_1}{S_{\nu 2}-\delta_2}$ instead of $\frac{S_{\nu 1}}{S_{\nu 2}}$, where δ_1 and δ_2 are the different fluxes subtracted or left out at the two frequencies owing to the inadequacies of the measurement methods.

Ryle (1952) developed his phase-switching interferometer to overcome the limitations arising from gain variations that affected the early additive interferometers. In this paper, we use his technique to convert a single dish to an *one-element interferometer* (OEI). This allows measuring only the cosmic emission without resorting to scanning, which has many notable advantages. In Section 2, we describe the basic method. In Section 3, we compute the expected ideal power beam of such an OEI. In Section 4, we discuss its implications for adding short-spacing data to interferometric data set. In Section 5, we discuss the advantages of OEI. Finally, we summarize the salient results of our investigation.

2 ONE-ELEMENT INTERFEROMETER

In his phase-switching interferometer, Ryle (1952) introduced an 180° phase switch in one of the legs of a two element additive interferometer. Millimeterwave Bolometric Interferometer and Einstein Polarization Interferometer for Cosmology use multiple horns, whose locations control the baselines, that receive, phase-shift and re-radiate into a telescope, which acts as a quasi-optical beam combiner and forms the image at the focal plane, measured using bolometric arrays (Timbie et al. 2006; Piat et al. 2012). In this work, we also introduce a phase shifter in the radio path but in a different way. For this, we notionally divide the aperture into two complementary subapertures and switch the phase shifter in and out of the rays reflected from only one of them. Then, applying the additive interferometer principle allows measuring the correlations between the two parts of the single aperture, converting a single dish into an OEI.

Consider two contiguous areas on the antenna (e.g. black and red areas shown in Fig. 2). Let x_1 and x_2 be the net signals received at the total power detector from these two areas of the primary. Consider switching in and out a half-wave delay element (HWDE) covering only the second (red) area. Introduction of HWDE makes that part of the incident signal inverted with respect to that reflected from

★ E-mail: ramesh@rri.res.in

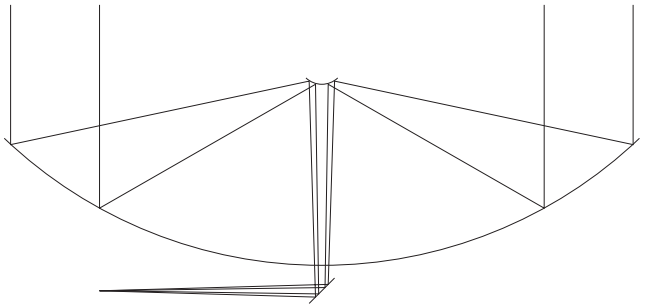

Figure 1. A conventional Nasmyth focus telescope with a paraboloidal primary, a hyperboloid secondary and a 45° plane mirror to bend the beam.

the other part. Therefore, the outputs measured by the total power detector in the two positions of the HWDE, in and out, are given by $V_1 = (x_1 - x_2)^2$ and $V_2 = (x_1 + x_2)^2$. The difference between these two measurements, $V_2 - V_1 = 4x_1x_2$, gives the correlation of the incident signal *between* the two contiguous areas on the dish. Switching the HWDE in and out at a rapid rate will completely cancel the common mode signals and yield a pure correlation output. To be precise, the HWDE has a characteristic wavelength λ_0. Around this wavelength, the correlation strength will fall-off cosinusoidally with frequency, ν: $V_2 - V_1 = 4x_1x_2\sin^2(2\pi\nu\lambda_0/4c)$. This fact can be used advantageously to adapt this concept for surface measurements but here it is suffice to note that over ± 5 per cent range around the central wavelength, the fall is $\lesssim 2$ per cent and therefore, insignificant. This means OEI has $\gtrsim 10$ per cent bandwidth: at 100 GHz, this is 10 GHz, similar to the current Atacama Large Millimetre-wave Array bandwidth.

One could also switch in and out a quarter-wave delay element (QWDE) instead of an HWDE. In that case, the outputs measured by the total power detector in the two positions of the QWDE, in and out, are given by $V_1 = (x_1^2 + x_2^2)$ and $V_2 = (x_1 + x_2)^2$. The difference between them, $V_2 - V_1 = 2x_1x_2$, gives the correlation of the incident signal *between* the two contiguous areas on the dish. Of course, the correlation strength falls to half that of the HWDE. Including the wavelength dependence, the correlation will be $V_2 - V_1 = 4x_1x_2\sin^2(2\pi\nu\lambda_0/8c)$. Over a 10 per cent bandwidth, the correlation varies nearly linearly.

We now present a simple way to implement this scheme in a conventional radio telescope. Consider a Nasmyth focus telescope with a paraboloidal primary, a hyperboloid secondary and a 45° plane mirror to bend the beam as shown in Fig. 1. Let us imagine the secondary to be divided into two parts: inner and outer. Then, we could arrange them in either of two configurations: (a) they both coincide with the ideal hyperboloidal surface; (b) the outer part displaced towards the rear focus by an amount, $\lambda/8$, and the inner part displaced away from the rear focus by the same amount; on reflection, this effectively produces a relative phase shift of $\lambda/2$ between the two parts of the wavefront and mimics inserting an HWDE. We can switch the secondary between these two configurations and thereby introduce the partial phase switching in time. Then, successive difference determined synchronously will yield the correlation similar to switching an HWDE in and out as discussed above. Alternately, we could implement a similar partitioning and switching scheme with the tertiary mirror. In this case, the tertiary should be in the far-field of the feed, so that its surface maps one-to-one on to the primary.

A natural question is, where to part? It is well known that one obtains maximum correlation between two telescopes with similar

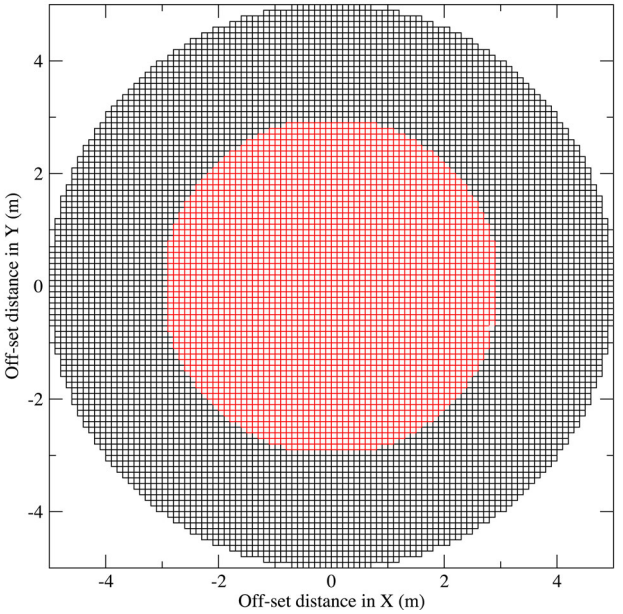

Figure 2. Gaussian-illuminated inner (red) and outer (black) areas of a 10 m telescope contributing equally to the received signal are shown gridded into 0.1 m square cells.

illumination when their areas are equal. In the case of OEI, for uniform illumination, the parting radii dividing the primary into 25, 50 and 75 per cent areas of illumination will be 50, 70.7 and 86.6 per cent of the dish radius, R. For Gaussian illumination of the form $e^{-(K/2)(r/R)^2}$, the fractional illumination, f_V, and its corresponding radius, f_r, are related by $f_r = \sqrt{-\frac{2}{K}\ln(1 - f_V\,(1 - e^{-K/2}))}$. Therefore, for $K = 4$, the parting radii corresponding to the above three fractions of illumination are 0.349, 0.532 and 0.724R, respectively. For single phase inversion, 180° phase difference is introduced between the two subapertures separated at 0.532R. For dual phase inversion, 180° phase difference is introduced between the odd and even of the four concentric subapertures separated at 0.349, 0.532 and 0.724R. In the next section, we compute the beam patterns for such single and dual phase inversion schemes. One could use more complex partitioning schemes such as dividing the circular aperture into multiple concentric annuli or several sectors or many small circles within the big outer one. By using such more complex shapes one can modify the spatial frequency response to suit the requirements at hand, but they may cause higher sidelobe levels and implementing them may be more difficult. Designing and implementing the partitioning pattern is an interesting and important task in making an OEI.

3 COMPUTING THE EFFECTIVE POWER BEAM

In this section, we compute the expected power beam pattern relevant for correlation signal obtained from successive differences of such configuration-switched total power data. The complex field distributions at the *aperture* and the *far-field* are Fourier related. For axisymmetric distributions, the radial field distributions at the *aperture* and the *far-field* are Hankel related. Therefore, one can Hankel-transform the radial field distribution without and with phase inversions to obtain the far-field voltage beam patterns. Squaring and finding the difference between them yield the effective power beam

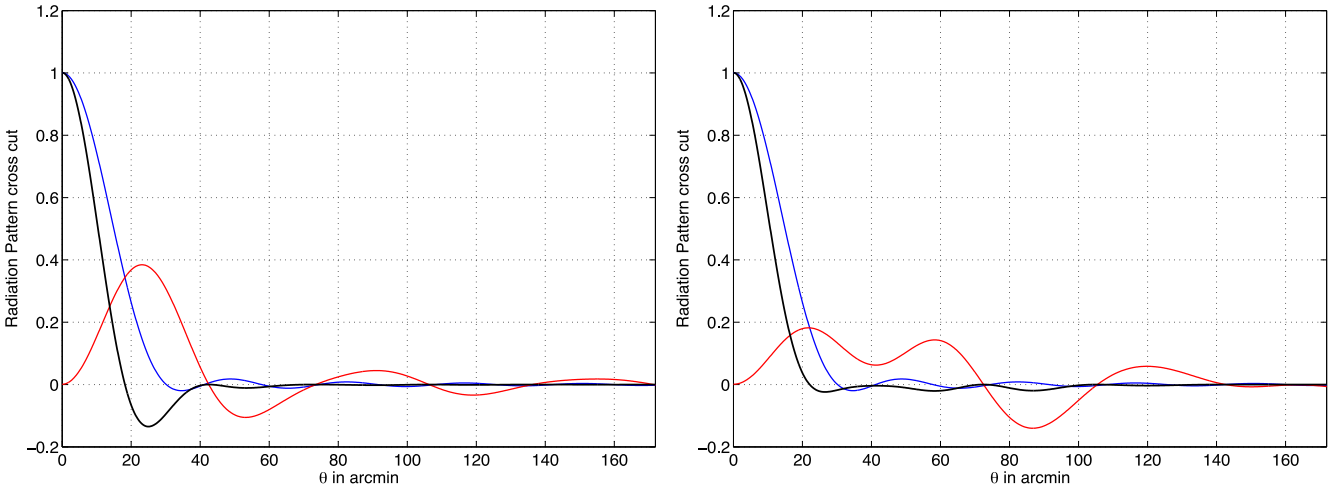

Figure 3. Radial cuts of the symmetric beam patterns for a voltage illumination of the form $e^{-2(r/R)^2}$. The left-hand panel is for single phase inversion with the parting radius at $f_r = 0.532$ and the right-hand panel for dual phase inversion with three parting radii at 0.349, 0.532 and 0.723. The blue and red curves are the voltage patterns for 0° and 180° switched configurations. The black curve is the power beam for the difference measurement. The single inversion has noticeable negative trough around the main beam. It is mitigated in dual inversion.

for the difference measurement. We have computed these for the two voltage beams and the resultant difference power beam for the two cases mentioned above, single and dual phase inversion. The radial cuts are shown in Fig. 3.

For, non-axisymmetric subaperture distributions (e.g. multiple small circles in a large outer circle), one can divide the aperture into many small cells and determine the cross-correlations between the cells among the subapertures and compute the UV weighting function. First, unique pairs of cells from each subaperture are formed. For each such pair, the product of their respective Gaussian weights are added to the $[u, v]$ cell, determined by the spacing between them. The Fourier transform of the UV weighting function thus obtained will yield the power beam pattern.

To validate this method, we apply it to a 10 m telescope, gridded into 0.1 m square cells, as shown in Fig. 2. Parting at $0.534R$ ensures that the Gaussian illuminated inner (red) and outer (black) areas contribute equally to the signal received from the source. A radial cut of the resultant axisymmetric visibility weighting function for single phase inversion is shown as the red curve in Fig. 4. Its Hankel transform yields a radial cut of the power beam, shown as the black curve in the same figure. This is nearly identical to the one in Fig. 3, validating this method for use in the case of non-axisymmetric subaperture distributions.

In the single inversion scheme, we adopted the 50 per cent illumination radius as the parting radius in order to maximize point source efficiency. One can choose different parting radius thereby losing this optimization but may gain in reducing the nearby negative troughs. Fig. 5 shows the power beams for different parting radii around the optimal one to demonstrate this possibility.

A Gaussian illuminated single dish in total power mode provides dominant weightage to spacings from 0 to $1R$. As seen in Fig. 4, OEI provides dominant weightage to spacings from 0.25 to $1R$ for single phase inversion. By its nature, OEI yields cross-power beam that *lacks* zero-spacing response. This should lead to negative power troughs around the main beam. The question is, how is this negative beam distributed? By distributing it over wider angles, one mitigates its effect on measuring large angular structures. This is evident from the fact that the nearby negative trough in the power beam

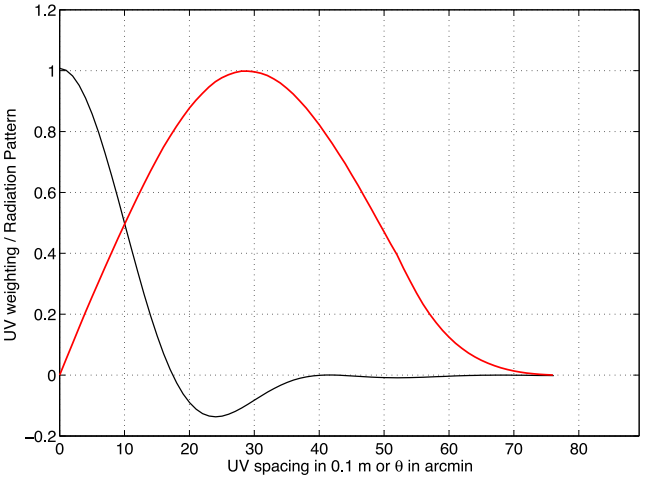

Figure 4. Radial cuts of the symmetric visibility weighting function (red) and its Hankel transform, the beam pattern (black). The latter is similar to the single inversion beam pattern in Fig. 3.

is dominant in single inversion but is mitigated in dual inversion. Other complex partitioning schemes may yield better results by shaping the short-spacing response appropriately. In summary, OEI will have resolving power similar to a single dish of the same size, but will differ in zero and very short spacing response.

The OEI output eliminates receiver contributions, especially if the configuration switching is done rapidly enough, say at 10 Hz. At centimetre wavelengths atmospheric emission is negligible, but at millimetre wavelengths it can be substantial. Atmospheric contributions to the total power output of a single dish are also dominated by self-correlations rather than cross-correlations, i.e. power is primarily contained in x_i^2 rather than in $x_i x_j$. This is why the correlation output of two nearby horns looking at a blank sky position yields zero mean, in the absence of a celestial source. Similarly, since the successive difference removes the self-correlations, OEI output will contain no atmospheric contributions and therefore no need to

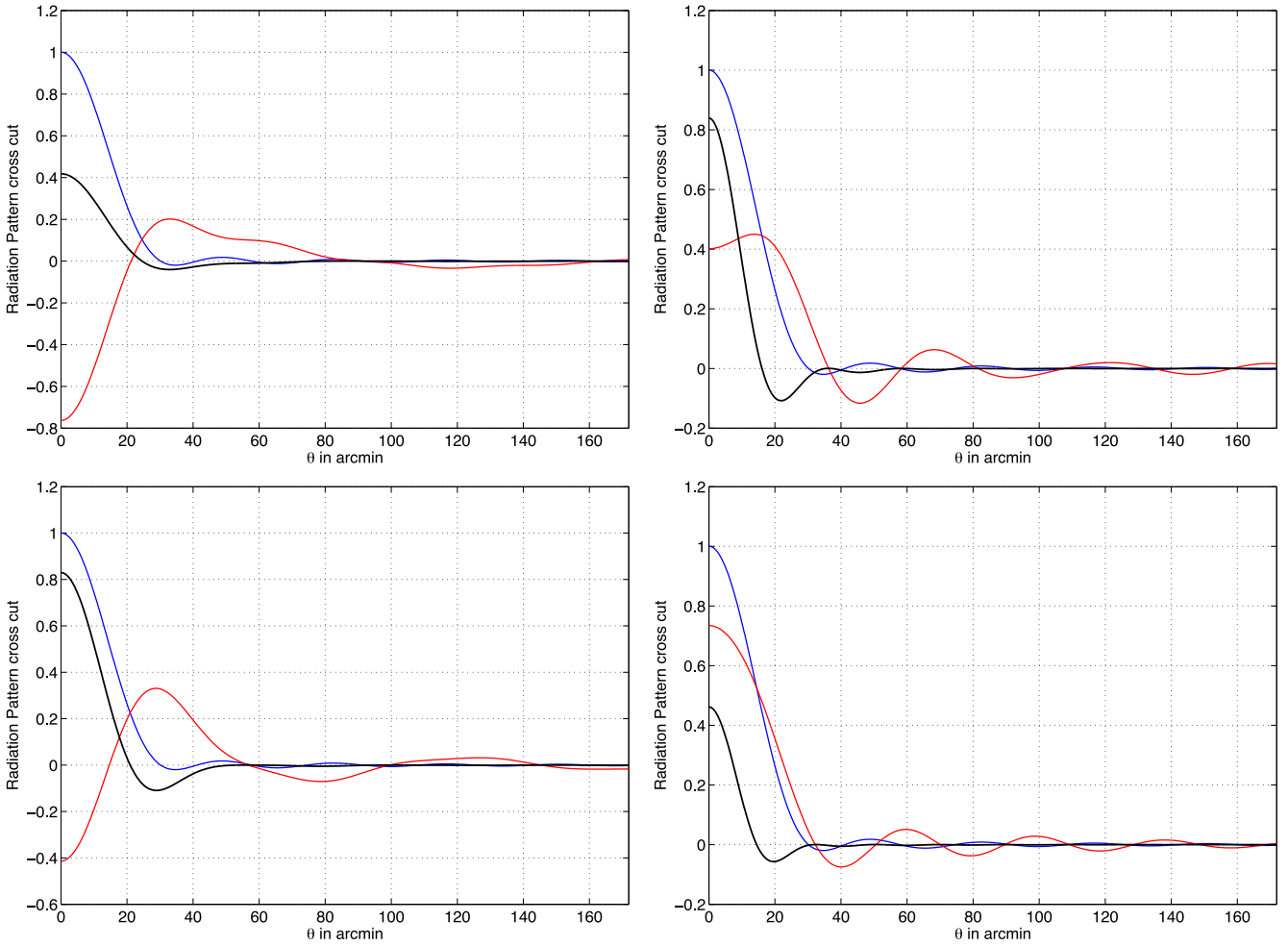

Figure 5. Radial cuts of the voltage beams and the difference power beam for a single phase inversion scheme, varying the partition radius. The left-hand panels are for radius 0.232 and 0.382*R*. The right-hand panels are for 0.682 and 0.832*R*. Changing the parting radius does change the short-spacing response and hence the negative troughs but at the cost of point source efficiency. Using multiple phase inversions is a better option.

resort to scanning techniques such as beam switching and basket weaving.

3.1 Sensitivity

OEI is as efficient as a single dish in beam switched mode. Of course, OEI continuously looks at the source unlike the latter. However, as mentioned above it uses only the cross-correlation between the two areas of the primary. This is equivalent to half the time loss or a signal loss by a factor of $1/\sqrt{2}$ in each of the switching configurations. Additionally, when they are synchronously differenced, the noise increases by a factor of $\sqrt{2}$. Thus, the overall signal-to-noise ratio (SNR) worsens by a factor of 2 similar to the beam-switching method. Basket-weaving and frequency-switching methods may provide better sensitivity for the same net observing time but, we believe, the OEI method will measure more accurately and with fewer assumptions. Further, OEI allows measurement of both spectral and continuum data, using coherent and bolometric arrays, and hence is a better switching method. We envisage that, once this technique is perfectly implemented and demonstrated, every single dish will have this as an additional observing mode.

4 OEI IN APERTURE SYNTHESIS

Converting one or more elements of a synthesis array to be OEIs should help adding short-spacing data to the visibilities in an easy and effective way. To cross-correlate OEI outputs with other elements, 180° switching may not be suitable as correlation strength drops to zero when HWDE is switched *in*. Instead, one should switch in and out a QWDE. Then, one could form a composite OEI output by multiplying it with the complex number $(1-j)$, i.e. by adding a 90° phase retarded copy with itself. When the QWDE is *out*, OEI output is $(x_1 + x_2)$ and the composite output is $(x_1 + x_2)(1 - j)$. Only the real part is in phase with the signal from the correlating antenna and therefore the orthogonal imaginary part drops out. When QWDE is *in*, the OEI output is $(x_1 + jx_2)$ and the composite output becomes $(x_1 + x_2) + j(x_2 - x_1)$. Again, only the real part is in phase with the signal from the correlating antenna and therefore the orthogonal imaginary part drops out. Thus, the composite OEI output behaves as an output from a regular single dish. Since the two signals being combined are orthogonal, when correlated with an output from another dish only the in-phase components get correlated and thereby one recovers full correlation strength of the OEI. Of course, in the process, the short-spacing component SNR becomes $1/\sqrt{8}$ of the raw SNR corresponding to the net observing

time. This may be sufficient because the short-spacing power from the source region may be several times stronger than at other spacings. Therefore, detecting the signal with other spacings may decide the overall integration time which will lead to good SNR to short-spacing data. If needed, more elements of the synthesis array may be operated in OEI mode to measure the short-spacing data, thereby compensating for the SNR loss owing to QWDE switching.

5 ADVANTAGES OF OEI

As seen above, OEI helps a single dish to avoid scanning and an array to extend its short-spacing response. In Section 2, we noted the frequency dependence of the correlation strength in OEI method. This fact can be used to measure the phase error caused by a part of the dish compared to an ideal paraboloid defined by the rest of the dish and thus determine the local surface deviation. For this purpose, a specially made phase-switching element is operated over the part under test. By moving this element around the dish mechanically one can measure the surface deviations at different locations. Elsewhere, we report in detail such a surface measurement method and its usefulness.

Ground-based IR observations too get limited by the sky-noise background from atmospheric emission. Fast switching methods are employed in order to mitigate their effects. Since OEI requires no scanning and, to a large extent, should remove the atmospheric emission, it may prove a useful observing tool. By appropriately masking a narrow region between the two subapertures that are correlated, one can filter-out low spatial frequencies, thereby imaging only compact emission. In this sense, OEI is like the nulling interferometer and may be helpful in studying, for example, Sun spots avoiding the Sun's disc. OEI may also be useful to overcome the SNR wall in spectrum sensing, important for Cognitive Radio (Tandra & Sahai 2008).

OEI may also yield the global or zero-spacing data. In the discussion so far, we only considered $V_2 - V_1$. We could also use any of the other three possible OEI outputs: V_1, V_2 and $V_2 + V_1$. Here, we outline how one may be able to retrieve the zero-spacing data using V_1. Imagine looking at a strong, isolated point source of known flux, in temperature unit, T K. The instantaneous gain will be $T/(V_2 - V_1)$, including e^{τ}, the correction factor for atmospheric loss. Noise injection at the receiver input can help to measure the rest of the receiver gain and thereby estimate the atmospheric opacity τ. The common mode signal, corrected for the atmospheric loss, in temperature unit is $TV_1/(V_2 - V_1)$. If the point source signal is completely cancelled, this will have the following components: T_0, $T_{\rm atm}$ and $T_{\rm sys}$. $T_{\rm sys}$ can be avoided using a correlation receiver or estimated accurately using load switching techniques. Using an atmospheric model and the opacity, $T_{\rm atm}$ can be estimated. Thus, in principle, V_1 may yield the zero-spacing data, T_0. Practical implementation will confirm if this is indeed possible.

In this work, we discussed only the use of phase switching between the two subapertures. One can also switch the polarization states in them. We are investigating such a scheme for a telescope with a dual polarization receiver.

6 SUMMARY

The phase-switching method of Ryle (1952) is applied to convert single dish radio telescopes to OEI. The output from such a telescope is expected to yield only spatially correlated signal on the source, both spectral and continuum, and to avoid receiver and atmospheric noise–power contributions. Such a system requires no scanning of the source and performs as well as a single dish in beam-switched observing mode. Converting one or more antennas of a synthesis array to operate as OEIs, preferably using QWDE switching, will allow adding reliable short-spacing correlation data to those arrays. OEI will also help ground-based NIR/MIR imaging by accurately removing atmospheric contributions. Finally, we note that the OEI concept allows one to use a small phase-switching element to measure local surface deviations of a paraboloidal dish.

ACKNOWLEDGEMENTS

Author thanks the Raman Research Institute and the Department of Science and Technology, India for their unwavering support to this research. Author also thanks the referee whose comments have improved the manuscript.

REFERENCES

Birkinshaw M., 1999, Phys. Rep., 310, 97
Carlstrom J. E., Holder G. P., Reese E. D., 2002, ARA&A, 40, 643
Cornwell T. J., 1988, A&A, 202, 316
Haslam C. G. T., Quigley M. J. S., Salter C. J., 1970, MNRAS, 147, 405
Jarosik N. et al., 2003, ApJS, 145, 413
Meinhold P. et al., 2009, J. Instrum., 4, 2009
Myers S. T., Baker J. E., Readhead A. C. S., Leitch E. M., Herbig T., 1997, ApJ, 485, 1
Piat M. et al., 2012, J. Low Temp. Phys., 167, 872
Ryle M., 1952, Proc. R. Soc. A, 211, 351
Sault R. J., Staveley-Smith L., Brouw W. N., 1996, A&AS, 120, 375
Tandra R., Sahai A., 2008, IEEE J. Sel. Top. Signal Process., 2, 4
Timbie P. T. et al., 2006, New Astron. Rev., 50, 999
Tiuri M., 1964, IEEE Trans. Antennas Propag., AP-12, 930
Winkel B., Flöer L., Kraus A., 2012, A&A, 547, A119
Woody D. P. et al., 2004, Proc. SPIE, 5498, 30

This paper has been typeset from a TEX/LATEX file prepared by the author.